

Shock wave and modelling study of the unimolecular dissociation of Si(CH₃)₂F₂: an access to spectroscopic and kinetic properties of SiF₂

C. J. Cobos¹, L. Sölter^{2, 3}, E. Tellbach^{2, 3},
and J. Troe^{2, 3, *}

Electronic Supplementary Information

¹ INIFTA, Facultad de Ciencias Exactas, Universidad Nacional de La Plata, CONICET, Argentina

² Institut für Physikalische Chemie, Universität Göttingen, Tammannstrasse 6, D-37077 Göttingen, Germany

³ Max-Planck-Institut für Biophysikalische Chemie, Am Fassberg 11, D-37077 Göttingen, Germany

* Email: juergen.troe@mpibpc.mpg.de

**ESI – 1 Modelling of oscillator strengths for UV absorptions of
SiF_x (x = 1 – 3)**

Table S1 Experimental absorption cross sections of SiF₂ (σ , base e, in cm²) at temperatures near 1600 and 3000 K (see main text).

λ / nm	σ (1600 K)/ 10 ⁻¹⁸ cm ²	σ (3000 K)/10 ⁻¹⁸ cm ²
200	1.0	-
210	4.5	-
215	19.0	19.0
222	24.5	20.5
230	15.5	16.0
235	8.4	11.0
240	3.0	-
245	1.0	-
250	0.5	-
255	0.5	-

Table S2 Wavelengths of UV- absorption maxima λ (in nm) and oscillator strengths f (determined by time-dependent density functional theory, TD-DFT, on the ω B97X-D level and with 6-311+G(3df) basis set; the calculations in **ESI – 1** and **ESI – 2** employed the Gaussian 09 software. revision – A.02-SMP, of ref. S1).

DFT model	λ (SiF ₃)	f (SiF ₃)	λ (SiF ₂)	f (SiF ₂)	λ (SiF)	f (SiF)
ω B97X-D	186	0.1259	225	0.1902	278	0.1104
	185	0.1259			218	0.0226
					195	0.0436

ESI – 2 Rate Constants of the unimolecular decomposition of Si(CH₃)₂F₂

a. Reaction enthalpies

All calculations were performed at the CBS-QB3 and G4 ab initio composite levels with geometries and harmonic vibrational frequencies derived at the B3LYP/6-311++G(3df,3pd) DFT level.

Table S3 Dissociation enthalpies of Si(CH₃)₂F₂ and Si(CH₃)F₂ (from CBS-Q//B3LYP/6-311++G(3df,3pd) and G4//B3LYP/6-311++G(3df,3pd) calculations, enthalpies at 0 K and in kJ mol⁻¹).

Reaction	CBS-Q//B3LYP/6-311++G(3df,3pd)	G4//B3LYP/6-311++G(3df,3pd)
Si(CH ₃) ₂ F ₂ → Si(CH ₃)F ₂ + CH ₃	410.0	401.7
Si(CH ₃)F ₂ → SiF ₂ + CH ₃	173.2	169.9

b. Properties of the potential energy surface along the minimum-energy path(MEP) for the reaction $\text{Si}(\text{CH}_3)_2\text{F}_2 \rightarrow \text{CH}_3 + \text{Si}(\text{CH}_3)\text{F}_2$

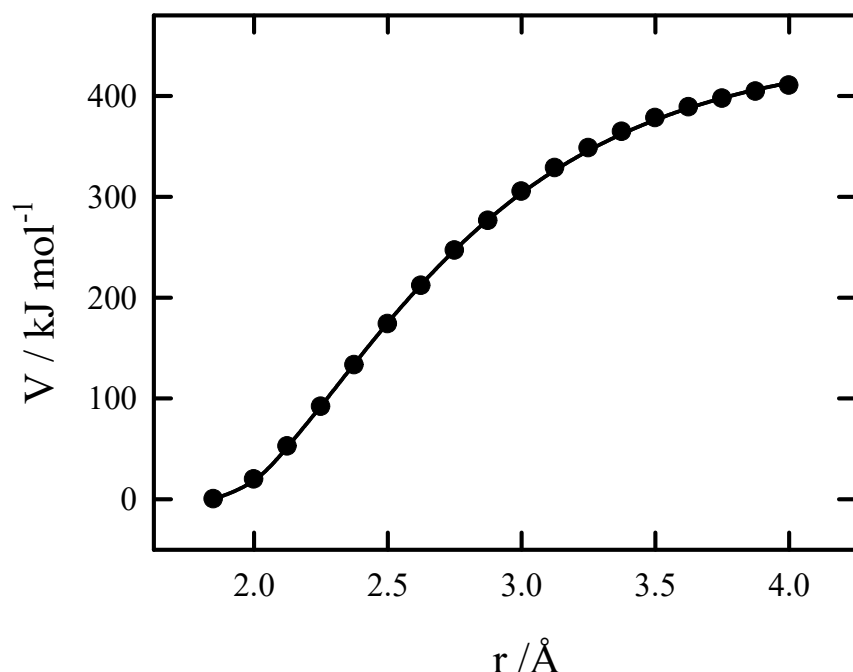


Fig. S1 Electronic potential for the reaction $\text{Si}(\text{CH}_3)_2\text{F}_2 \rightarrow \text{CH}_3 + \text{Si}(\text{CH}_3)\text{F}_2$ along the MEP. G4//B3LYP/6-311++G(3df,3pd) calculations fitted with a Morse function with $D_e = 447.3 \text{ kJ mol}^{-1}$ and $\beta = 1.51 \text{ \AA}^{-1}$

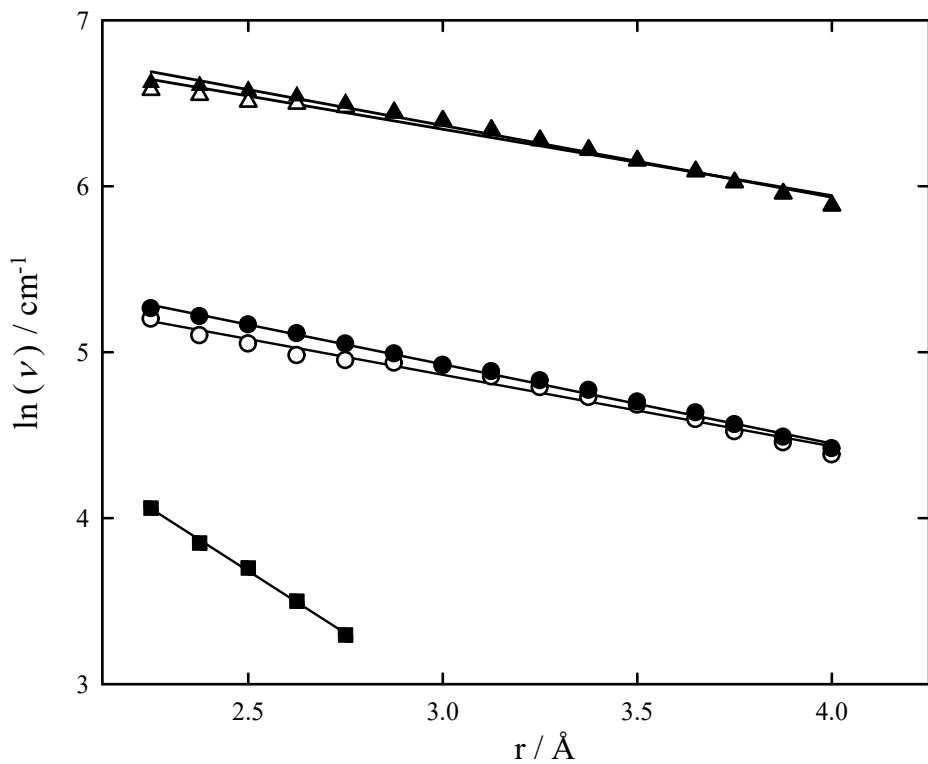


Fig. S2 Transitional modes ν of the reaction $\text{Si}(\text{CH}_3)_2\text{F}_2 \rightarrow \text{CH}_3 + \text{Si}(\text{CH}_3)\text{F}_2$ along the MEP, calculated at the B3LYP/6-311++G(3df,3pd) level. Exponential decay functions with decay parameters $\alpha = 1.50$ (■), 0.43 (○), 0.48 (●), 0.40 (Δ) and 0.43 \AA^{-1} (\blacktriangle).

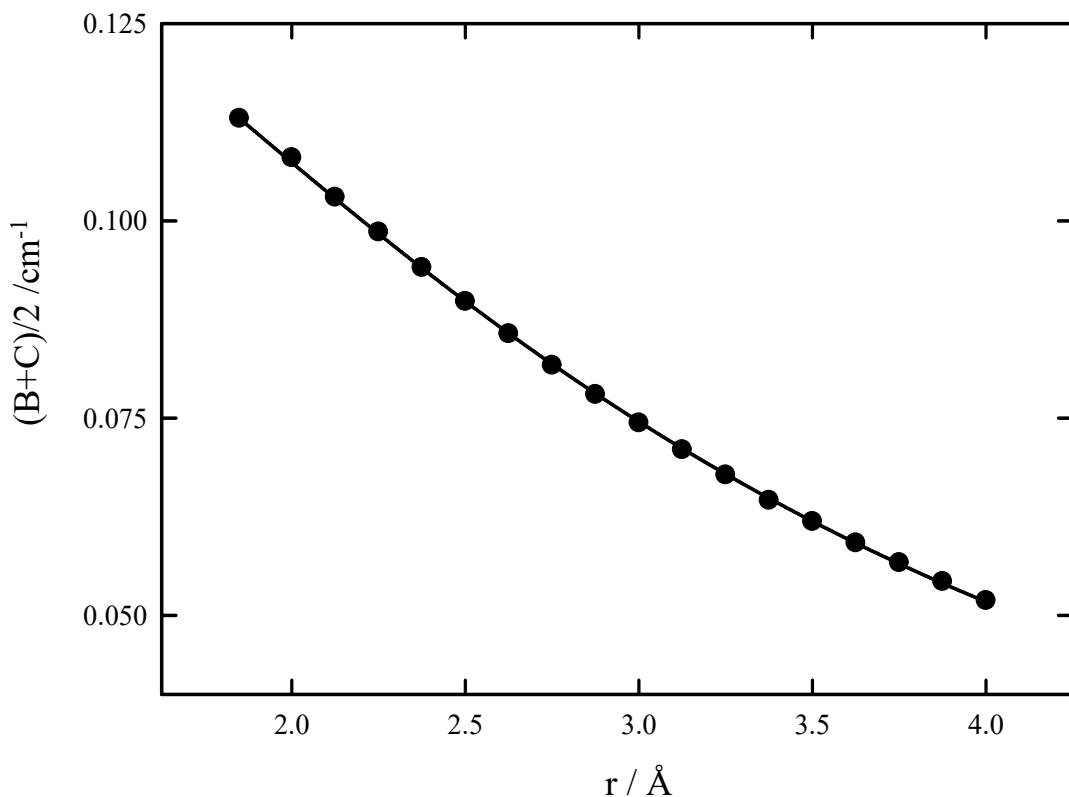


Fig. S3 Rotational constants of $\text{Si}(\text{CH}_3)_2\text{F}_2$ calculated along the MEP for the reaction $\text{Si}(\text{CH}_3)_2\text{F}_2 \rightarrow \text{CH}_3 + \text{Si}(\text{CH}_3)\text{F}_2$, calculated at the B3LYP/6-311++G(3df,3pd) level (fit with a function $(\text{B}+\text{C})/2 = 0.113 \text{ cm}^{-1} / [1 + 0.330(r - 1.849) + 0.103(r - 1.849)^2]$).

c. Modelling of limiting high pressure rate constants

Table S4 Modelled limiting rate high pressure constants for the recombination reaction $\text{CH}_3 + (\text{CH}_3)\text{SiF}_2 \rightarrow (\text{CH}_3)_2\text{SiF}_2$ ($k_{\text{rec},\infty}$, in $\text{cm}^3 \text{ mol}^{-1} \text{ s}^{-1}$) and the reverse dissociation reaction $\text{Si}(\text{CH}_3)_2\text{F}_2 \rightarrow \text{CH}_3 + \text{Si}(\text{CH}_3)\text{F}_2$ (k_∞ , in s^{-1}) (calculations with the simplified statistical adiabatic channel/classical trajectory model, SACM/CT, of ref. S2 and S3, employing the parameters of Figs. S1 - S3, PST = phase space theory, rigidity factors $f_{\text{rigid}} = k_{\text{rec},\infty} / k_{\text{rec},\infty}^{\text{PST}}$, equilibrium constants $K_c = k_\infty / k_{\text{rec},\infty}$, in mol cm^{-3}).

T/K	$k_{\text{rec},\infty}^{\text{PST}}$	f_{rigid}	$k_{\text{rec},\infty}$	K_c	k_∞
1500	3.65×10^{14}	5.05×10^{-2}	1.84×10^{13}	5.62×10^{-11}	1.03×10^3
1750	3.84×10^{14}	5.13×10^{-2}	1.97×10^{13}	4.91×10^{-9}	9.66×10^4
2000	3.98×10^{14}	5.20×10^{-2}	2.07×10^{13}	1.25×10^{-7}	2.58×10^6
2500	4.21×10^{14}	5.30×10^{-2}	2.23×10^{13}	9.04×10^{-6}	2.02×10^8

$$k_\infty = 1.24 \times 10^{19} (T/2000 \text{ K})^{-6.63} \exp(-58400 \text{ K}/T) \text{ s}^{-1}$$

d. Modelling of limiting low pressure rate constants

Table S5 Modelled limiting low pressure rate coefficients (k_0 , in $\text{cm}^3 \text{ mol}^{-1} \text{ s}^{-1}$) for the reaction $\text{Si(CH}_3)_2\text{F}_2 (+ \text{Ar}) \rightarrow \text{CH}_3 + \text{Si(CH}_3)\text{F}_2 (+ \text{Ar})$ (strong collision rate coefficients k_0^{SC} , calculated following ref. S4 and employing the parameters of Figs. S1 – S3; weak collision efficiencies $\beta_c = k_0 / k_0^{\text{SC}}$, as following from the master-equation treatment of ref. S5, were determined with assumed standard values of average energies transferred per collision of $\langle \Delta E \rangle = -100/\text{hc cm}^{-1}$).

T/K	k_0^{SC}	β_c	k_0
1500	1.18×10^{12}	0.038	4.49×10^{10}
1750	1.24×10^{13}	0.028	3.46×10^{11}
2000	4.88×10^{13}	0.021	1.02×10^{12}
2500	1.71×10^{14}	0.011	1.89×10^{12}

$$k_0 = [\text{Ar}] 2.94 \times 10^{25} (T/2000 \text{ K})^{-25.04} \exp(-61980 \text{ K}/T) \text{ cm}^3 \text{ mol}^{-1} \text{ s}^{-1}$$

e. Modelling of falloff curves

Falloff curves for the reaction $\text{Si(CH}_3)_2\text{F}_2 (+ \text{Ar}) \rightarrow \text{CH}_3 + \text{Si(CH}_3)\text{F}_2 (+ \text{Ar})$ were represented in the representation proposed in ref. S6 – S8 (see main text), employing center broadening factors F_{cent} estimated according to ref. S8 and leading to values of $F_{\text{cent}} = 0.039$ (1500 K), 0.045 (1750 K), 0.051 (2000 K) and 0.073 (2500 K).

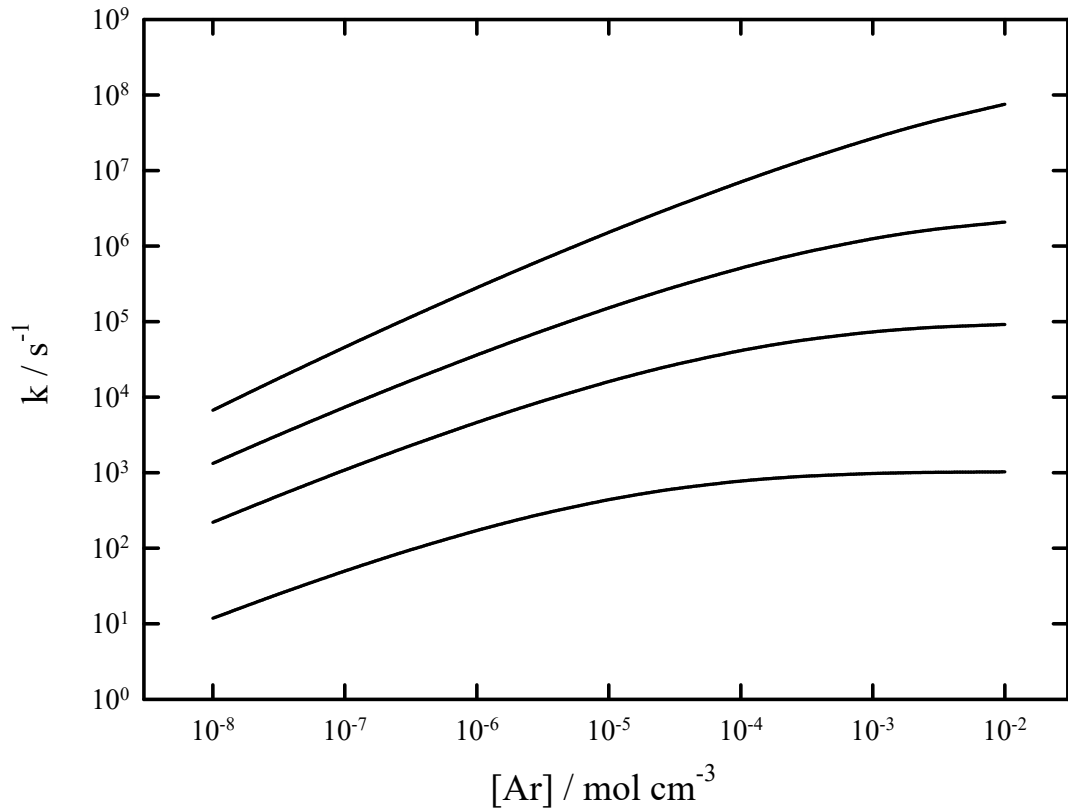


Fig. S4 Modelled falloff curves for $\text{Si}(\text{CH}_3)_2\text{F}_2$ (+ Ar) $\rightarrow \text{CH}_3 + \text{Si}(\text{CH}_3)\text{F}_2$ (+ Ar). Calculations for 1500, 1750, 2000 and 2500 K (from bottom to top).

f. Molecular parameters

Bond dissociation enthalpy for $\text{Si}(\text{CH}_3)_2\text{F}_2 \rightarrow \text{CH}_3 + \text{Si}(\text{CH}_3)\text{F}_2$ at 0 K: $\Delta H_0^0 = 401.7 \text{ kJ mol}^{-1}$ (from G4//B3LYP/6-11++G(3df,3pd) calculations).

$\text{Si}(\text{CH}_3)_2\text{F}_2$ vibrational frequencies: 141, 153, 193, 210, 250, 320, 322, 635, 707, 758, 789, 801, 828, 905, 930, 1307, 1309, 1453, 1455, 1462, 1465, 3034, 3036, 3106, 3109, 3111, 3111 cm^{-1} (from B3LYP/6-311++G(3df,3pd) calculations).

$\text{Si}(\text{CH}_3)_2\text{F}_2$ rotational constants: A = 0.126, B = 0.114, C = 0.112 cm^{-1} ($\sigma = 2$) (from B3LYP/6-311++G(3df,3pd) calculations).

$\text{Si}(\text{CH}_3)\text{F}_2$ vibrational frequencies: 130, 213, 271, 324, 635, 774, 778, 846, 897, 1270, 1441, 1454, 3029, 3112, 3131 cm^{-1} (from B3LYP/6-311++G(3df,3pd) calculations).

$\text{Si}(\text{CH}_3)\text{F}_2$ rotational constants: A = 0.231, B = 208, C = 0.123 cm^{-1} ($\sigma = 1$) (from B3LYP/6-311++G(3df,3pd) calculations).

CH_3 vibrational frequencies: 541, 1407, 1407, 3111, 3289, 3289 cm^{-1} (from B3LYP/6-311++G(3df,3pd) calculations).

CH_3 rotational constants: A = 9.601, B = 9.601, C = 4.800 cm^{-1} ($\sigma = 3$) (from B3LYP/6-311++G(3df,3pd) calculations).

Lennard-Jones parameters: $\sigma(\text{Si}(\text{CH}_3)_2\text{F}_2) \approx \sigma(\text{SiF}_4) = 4.88 \text{ \AA}$ and $\varepsilon/k(\text{Si}(\text{CH}_3)_2\text{F}_2) \approx \varepsilon/k(\text{SiF}_4) = 171.9 \text{ K}$ (from ref. S9); $\sigma(\text{Ar}) = 3.47 \text{ \AA}$, $\varepsilon/k(\text{Ar}) = 114 \text{ K}$ (from ref. S10).

g. References

- (S1) Gaussian 09, revision A.02-SMP, M. J. Frisch, G. W. Trucks, H. B. Schlegel, et al. (Gaussian Inc., Wallingford CT, 2009).
- (S2) A. I. Maergoiz, E. E. Nikitin, J. Troe, V. G. Ushakov, Classical trajectory and statistical adiabatic channel study of the dynamics of capture and unimolecular bond fission. V. Valence interactions between two linear rotors, *J. Chem. Phys.* 108 (1998) 9987 – 9998.
- (S3) A. I. Maergoiz, E. E. Nikitin, J. Troe, V. G. Ushakov, Classical trajectory and statistical adiabatic channel study of the dynamics of capture and unimolecular bond fission. VI. Properties of transitional modes and specific rate constants k(E, J), *J. Chem. Phys.* 117 (2002) 4201 - 4213.
- (S4) J. Troe, Predictive possibilities of unimolecular rate theory, *J. Phys. Chem.* 83 (1979) 114 – 126.
- (S5) J. Troe, Theory of thermal unimolecular reactions at low pressures: I. Solutions of the master equation, *J. Chem. Phys.* 66 (1977) 4745 – 4757.
- (S6) J. Troe, V. G. Ushakov, Revisiting falloff curves of thermal unimolecular reactions, *J. Chem. Phys.* 135 (2011) 054304.
- (S7) J. Troe, V. G. Ushakov, Representation of “broad” falloff curves for dissociation and recombination reactions, *Z. Phys. Chem.* 228 (2013) 1 – 10.
- (S8) J. Troe , Theory of thermal unimolecular reactions in the falloff range. I. Strong collision rate constants, *Ber. Bunsenges. Phys. Chem.* 87 (1983) 161 – 169.

- (S9) TRA-036-1 Chemkin Collection Release 3.6 September 2000, A software package for the evaluation of gas-phase multicomponent transport properties,
[https://www3.nd.edu/~powers/ame.60636\(transport.pdf\)](https://www3.nd.edu/~powers/ame.60636(transport.pdf)).
- (S10) H. Hippler, H. J. Wendelken. J. Troe, Collisional deactivation of vibrationally highly excited polyatomic molecules. II. Direct observations for excited toluene, *J. Chem. Phys.* 78 (1983) 6709 – 6717.